Amine Functionalized Kit-6 Mesoporous Magnetite Nanocomposite as an Efficient Adsorbent for Removal of Ponceau 4R Dye from Aqueous Solutions

M. Sojoudi, S. Shariati* and M. Khabazipour

Department of Chemistry, Rasht Branch, Islamic Azad University, Rasht, Iran
(Received 15 January 2016, Accepted 2 August 2016)

In this study, amine functionalized Kit-6 silica mesoporous magnetite nanocomposite (NH_2-MMNC) was synthesized by chemical methods and used as an efficient and recoverable adsorbent for removal of Ponceau 4R, as a toxic dye, from aqueous solutions. The synthesized nanocomposites were characterized by XRD, FT-IR, BET and SEM instruments. The effect of various experimental parameters on the dye removal efficiency was studied using Taguchi orthogonal array design (L_9 array) method. Under optimum conditions (pH = 2, adsorbent amount = 80 mg, stirring time = 30 min and without addition of salt), removal efficiency was obtained higher than 98%. The kinetic studies showed rapid sorption dynamics by a second-order kinetic model with $R^2 = 0.9993$ and $q_{eq} = 58.8$ mg g^{-1}, suggesting chemisorption mechanism. Dye adsorption equilibrium data were fitted well to the Langmuir isotherm and the synthesized sorbent showed complete removal efficiency. The maximum monolayer capacity of the sorbent (Q_{max}, mg g^{-1}), and the Langmuir binding constant related to the energy of adsorption (K_L, l mg^{-1}), were obtained 87.7 and 0.407, respectively. The results of real samples show that the synthesized nanocomposite can be used as a recyclable and efficient adsorbent for removal of Ponceau 4R anionic dye from aqueous solutions.

Keywords: Kit-6 mesoporous magnetite nanocomposite, Amine-functionalized, Ponceau 4R, Dye removal

INTRODUCTION

The supervision of food additives is a big concern in most countries because most of these chemicals are carcinogenic and poisonous. Between different food additives, synthetic colorants have been extensively used to make food more attractive and charming. Nevertheless, some of synthetic dyes can be particularly pathogenic if they are too much consumed [1,2]. Dyes are widely used as colorant in drug, cosmetic and food industries to produce dyeing sweets, chewing gums, juices, puddings, mustard, drugs and cosmetics [3]. Ponceau 4R, known as E124 or Acid Red 18, is a synthetic food dye that is classified as a strong acid dye. The FAO/WHO Joint Expert Committee on Food Additives formulated acceptable daily intake values for Ponceau 4R and other azo dyes and many other

countries banned its usage in food. Nevertheless, Ponceau 4R is yet consumed as a coloring matter in medicines, drinks, food, tobacco and cosmetic industries in many countries. The natural dye originates from cochineal, but lately nearly whole the Ponceau 4R has been synthesized. Excessive consumption of Ponceau 4R cause mutagenic and carcinogenic impacts [4]. Because the dyes are not completely fixed on the products, the food industries generate dye-containing effluents [5]. Nevertheless, about 10-20% of the dyes are lost during production process, leadings to plenty amounts of wastewater [6]. The improper diffusion of dye-containing wastewater is aesthetically in appropriate and can cause several direct and indirect effects on the human health and environment [7-9]. The colored wastewaters are very hard to be treated, because colors are resistant molecules against aerobic digestion. For this reason, numerous traditional treatment methods including membrane filtration, precipitation, coagulation, photo

_____
*Corresponding author. E-mail: Shariaty@iaurasht.ac.ir

degradation, oxidation, and adsorption have been used to eliminate or remove dyes from wastewaters. Especially, adsorption process is considered to be an effective and economical procedure for removal of dyes from industrial wastewaters [10,11]. For the past decade, many efforts have been assigned for design and synthesis of nanostructured sorbents [12]. In comparison with the micron-sized conventional sorbents, nano-sized particles, especially Fe_3O_4 magnetite nanoparticles (MNPs), possess advantages of large surface area and high magnetic properties, which cause high adsorption efficiency, high removal rate of contaminants, and easy and rapid separation of adsorbent from solution via an external magnetic field. After magnetic separation, the contaminants can be easily separated from MNPs by the desorbent agents, and the recovered MNPs can be reused [13]. In last decade, magnetite nanoparticles have been used for some organic and inorganic pollutants without and after surface modification [12-16].

As far as our knowledge, there is no document about the removal of Ponceau 4R from aqueous samples by magnetite nanoparticles. Therefore, in the present research, the removal of Ponceau 4R azo dye from aqueous solutions using amine functionalized Kit-6 silica mesoporous magnetite nanocomposite (NH2-MMNC, Fe_3O_4@SiO_2@ Kit-6-NH2) is investigated. At acidic pHs, amino groups of NH2-MMNC have positive charges and can be linked to anionic Ponceau 4R *via* electrostatic interaction and separate it from solution. The effects of various experimental parameters on the sorption capacity of synthesized nanocomposites have been studied *via* Taguchi orthogonal array design (L9 array). The kinetic and isotherm models were investigated to show the rate and capacity of sorption process.

EXPERIMENTAL

Chemicals and Apparatus

Ponceau 4R (Fig. 1) with a dark red color and full chemical description of 1,3-naphthalenedisulfonic acid, 7-hydroxy-8-[(4-sulfo-1-naphthalenyl) azo] trisodium salt was prepared with analytical grade purity. Ferric chloride hexa hydrate ($FeCl_3.6H_2O$), ferrous chloride tetra hydrate ($FeCl_2.4H_2O$), ammonia (25% w/w), hydrochloric acid (37% w/w), absolute ethanol, sodium chloride, tetraethyl
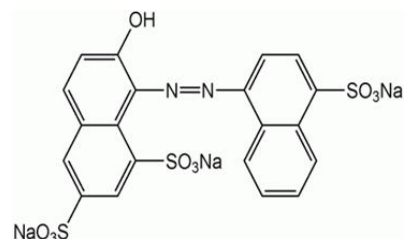

Fig. 1. Molecular structure of Ponceau 4R.

orthosilicate (TEOS), Pluronic P123 (EO_{20}-PO_{70}-EO_{20}, MW = 5800), 1-butanol, p-toluenesulfonic acid, 3-aminopropyl triethoxysilane (APTES) and toluene were prepared with high purity from Merck, Fluka and Sigma-Aldrich chemical companies. XRD pattern of the synthesized NH2-MMNC was obtained using X-ray diffraction (XRD) with 2θ range of 0.5-70° on X-PRTPRO (PANalitical, Netherland). Surface morphology of the modified nanoparticles was observed under a Philips XL 30 scanning electron microscope (SEM; the Netherlands). FT-IR instrument (Shimadzu FT-IR-470, Japan) was used in the range of 400-4000 cm^{-1} to investigate the chemical structure of the synthesized NH2-MMNCs. Nitrogen adsorption-desorption experiments were carried out at 77 K on a Belsorpmini II accelerated surface area and porosimetry system (Bel, Japan). The Brunauer-Emmett-Teller (BET) surface area (SBET) was calculated from the linearity of the BET equation. The surface area, volume and pore diameter of the synthesized MNPs were calculated from pore size distribution curves using the Barrett-Joyner-Halenda (BJH) formula. For spectrophotometric absorption measurements Mapada UV-Vis spectrophotometer (6300 PC, China) was used. pH of the solutions was adjusted using a Crison pH meter (Basic 20, Spanish). For magnetic separations, a strong super magnet with 1.4 T magnetic field (1 × 3 × 5 cm) was applied.

Synthesis of NH2-MMNC

The synthesis of KIT-6 mesoporous magnetite was performed according to the method reported in our previous work [12]. Briefly, MNPs were chemically synthesized with addition of deoxygenated aqueous solution of ferrous and ferric ions (in a 1:2 molar ratio) to 250 ml of degassed ammonia solution (1.5 M) using a dropping funnel during

60 min under nitrogen gas protection. During the whole process, the solution temperature was maintained at temperatures higher than 80 °C and the solution was stirred vigorously. After completion of the reaction, the obtained MNPs were separated from the reaction medium by a super magnet and then washed three times with 500 ml double distilled water and finally were dried at 90 °C for 120 min. Silica layer was coated on the surface of MNPs to form $Fe_3O_4@SiO_2$ nanoparticles and to protect MNPs from acidic condition. Briefly, 1.0 g of the synthesized MNPs was homogeneously dispersed in 500 ml of ethanol containing 5% (v/v) ammonia (25% w/w), under stirring at 80 °C followed by dropwise addition of ethanolic solution of TEOS (10.8% v/v). After 2 h stirring at 80 °C, the $Fe_3O_4@SiO_2$ nanoparticles were obtained and washed several times with a 1:1 mixture of water-ethanol and dried at 100 °C for 5 h to form dark brown MNPs-SiO_2.

The Kit-6 mesoporous silica with cubic Ia3d symmetry as shell on the magnetite core was synthesized using non-ionic surfactant of Pluronic P123 as structure conducting and TEOS (as silica source). For this purpose, 1.25 g Pluronic P123 was dissolved in 45 ml deionized water. Then, 1 g of MNPs- SiO_2, 2.4 ml of HCl (37 wt%) and 1.3 g of *n*-butanol (99.4 wt%) were added to the solution under vigorous stirring. After 1 h, 2.7 g of TEOS was added immediately and the mixture was stirred at 35 °C for 24 h. So, it was autoclaved at 100 °C for 24 h and the produced solid (MMNC) was filtered, washed and calcined at 550 °C for 6 h. For each 1.0 g MNP, 2.3 g MMNC was obtained.

Synthesis of NH$_2$-MMNC was carried out by the post-synthesis grafting method based on the silylation of organo alkoxysilane with surface silanol groups on the mesopores. For synthesis of NH$_2$-MMNCs, 0.5 g of the synthesized MMNCs was dispersed in 75 ml of toluene and stirred for 0.5 h at 50 °C. After that, 3.5 mg of *p*-toluene sulfonic acid and 1.0 mmol of APTES were added to the mixture and heated up to 120 °C and stirred (4 h). After refluxing (4 h), the solid product was filtered and washed with absolute ethanol several times and dried at 100 °C (12 h).

RESULTS AND DISCUSSION

Characterization of MNPs

FT-IR spectra of $Fe_3O_4@SiO_2@Kit-6$ (MMNCs) and $Fe_3O_4@SiO_2@Kit-6-NH_2$ (NH$_2$-MMNC) are shown in Fig. 2. IR spectra showed bands at ~557-565 and 439-460 cm^{-1} attributed to the Fe-O vibration of Fe_3O_4 in tetrahedral and octahedral sites, respectively. Also, the peak at ~1049-1070 cm^{-1} is attributed to the asymmetric stretching vibrations of Si-O-Si. Stretching vibration of the N-H functionalities was observed at 3429 cm^{-1}. The XRD patterns of MMNCs in Fig. 3 showed peaks with 2θ at 1 and 1.83 for Kit-6 (A), 0.89 and 1.76 for MMNC (B) indicating well resolved (211) and (332) peaks which are typical for cubic order materials with *la3d* space group. Other peaks with 2θ at 26.05, 30.315, 35.66, 43.35, 53.8, 57.3, 62.96 and 71.51 correspond to Fe_3O_4.

Nitrogen adsorption-desorption isotherm of the MMNCs showed a characteristic type IV curve with a distinct hysteresis loop in the p/p° range of 0.6-0.9, indicating the presence of a narrow distribution of mesoporous pore size. The type IV isotherm (IUPAC classification) is typical for mesoporous systems. The typical BJH (Barrett-Joyner-Halenda) pore size distributions showed narrow pore size distributions for samples. BET surface area (S_{BET}, m^2 g^{-1}), mean volume of the pores (V_p, cm^2 g^{-1}), mean pore diameter from BJH (d_o, nm) and surface area of pores (a_p, m^2 g^{-1}) for the synthesized MMNPs were obtained as 241.68, 0.566, 9.25 and 224.84, respectively. The results clearly indicate high surface area and large and uniform pores for the core/shell structure of MMNPs. Therefore, it can be deduced that the pores of the silica mesoporous shell remain after loading on the surface of iron oxide nanoparticles.

SEM images in Fig. 4 showed that the morphologies are very uniform and spherical nanoparticles with diameters about 17 nm have been synthesized.

Removal of Ponceau 4R Using NH$_2$-MMNCs

In order to find the maximum absorption wavelength of Ponceau 4R, the absorption spectra of dye was obtained in the range of 200-700 nm and 505 nm was selected as the best wavelength for quantitative measurements. All adsorption experiments were conducted at room temperature and the amount of adsorbed dye was estimated from the difference between initial and final dye concentrations in the solution. The removal efficiency of dye was calculated as:
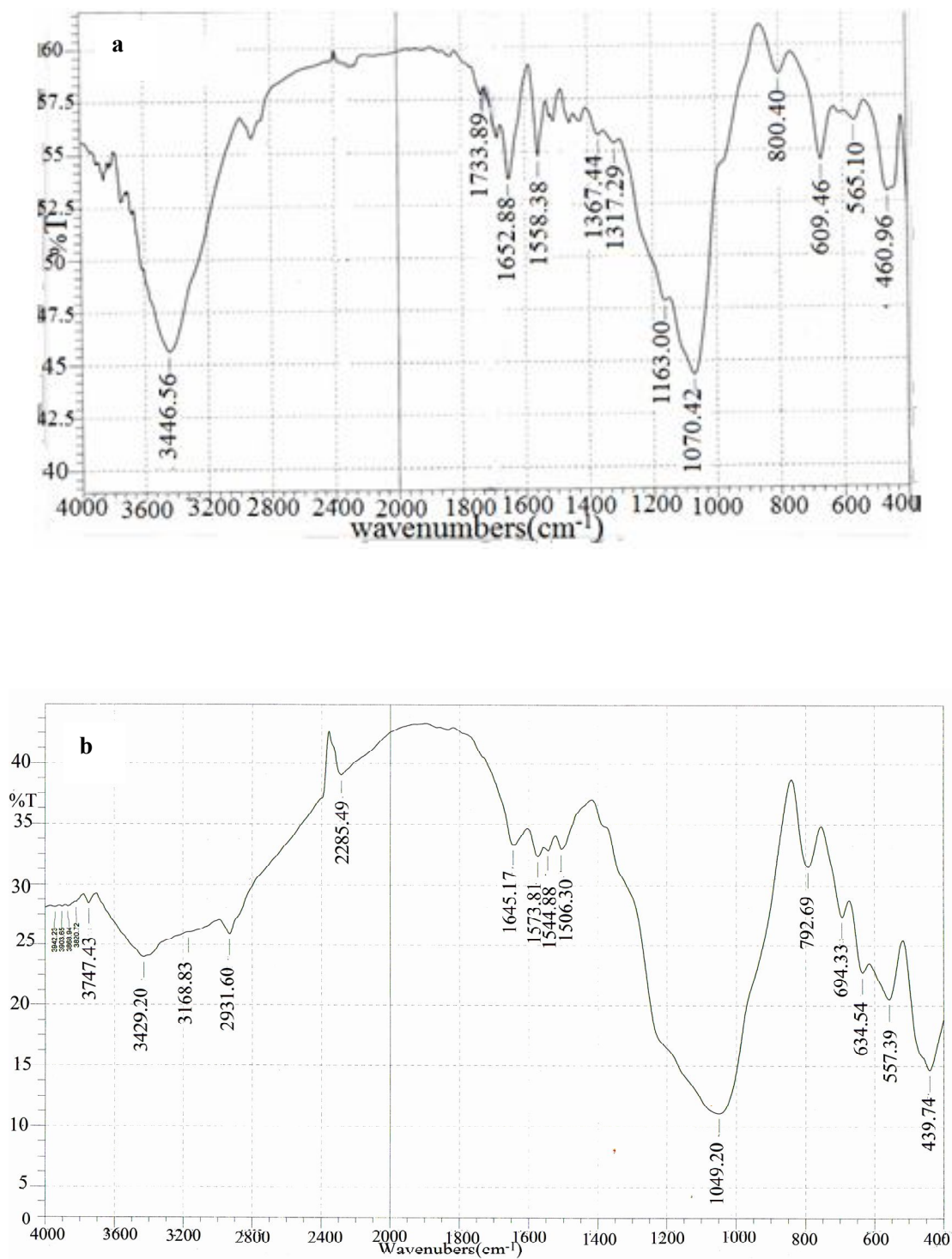
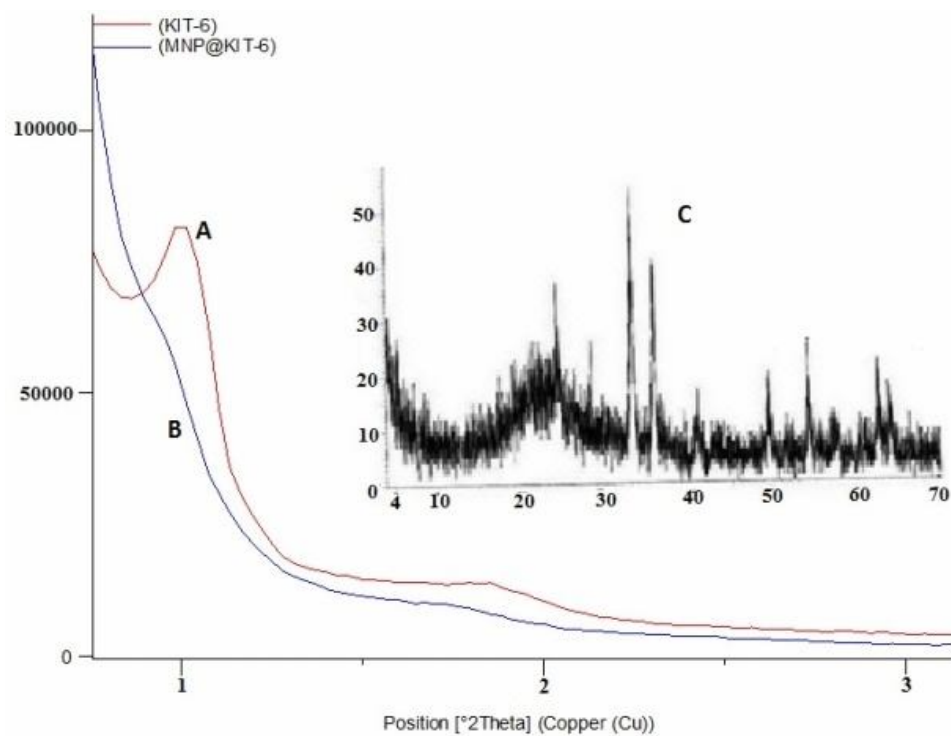**Fig. 2.** FT-IR spectra of (a) MMNCs (b) NH$_2$-MMNCs.

Fig. 3. X-Ray diffraction pattern of (A) Kit-6 (without magnetite core) (B) MMNCs in small angle (C) MMNCs in wide angle.
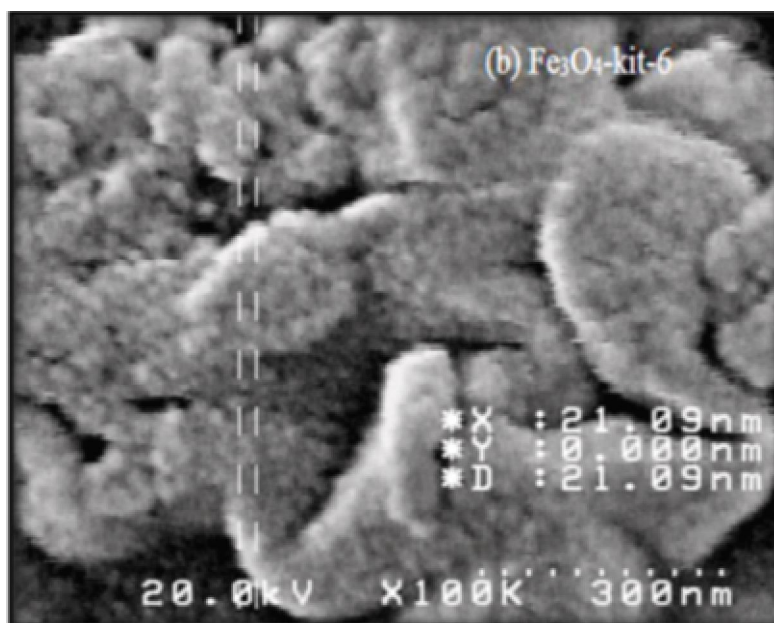

Fig. 4. SEM photographs of the MMNCs.

$$\% \mathrm{Re}\,moval = \frac{C_0 - C_t}{C_0} \times 100 \qquad (1)$$

where, C_o and C_t are initial and equilibrium concentrations of Ponceau 4R after treatment with adsorbent, respectively. In the proposed procedure, to achieve maximum sorption efficiency various parameters affecting the removal efficiency including sorbent weight, ionic strength, agitation time and pH of sample were studied and optimized with Taguchi orthogonal array design using L_9 array (4 factors at 3 levels) (Table 1). Taguchi method as an orthogonal array design was selected to minimize the number of optimization experiments and to show the influence of each experimental factor on the removal efficiency. According to the results of 9 experiments and the ANOVA calculations, the optimal conditions (for 50 ml of sample containing 50 mg l^{-1} of Ponceau 4R) were obtained.

Figure 5 shows a schematic diagram of the magnetic separation process for the removal of Ponceau 4R.

Effect of agitation time on the removal efficiency of Ponceau 4R. The influence of agitation time on the dye removal efficiency of NH$_2$-MMNCs was studied in the agitation time of 8, 15 and 30 min. By increasing stirring time from 8 to 30 min, the removal efficiency was improved from 24 to 57%. According to the results, contact time of 30 min was selected for further experiments.

Effect of adsorbent amount on the removal efficiency of Ponceau 4R. Adsorbent mass is a significant parameter to specify the capacity of an adsorbent for a given amount of the adsorbent at the operating conditions. Overlay, the color removal rate increases with increasing consumption of sorbent, where the quantity of sorption sites at the surface of adsorbent will increase by increasing the amount of the adsorbent. The influence of adsorbent dosage gives one, an idea to adsorb dye with a least amount of adsorbent, from an economical point of view [17]. The effect of the NH$_2$-MMNCs amount on the adsorption of dye was studied with 10, 40 and 80 mg of NH$_2$-MMNCs and 80 mg was selected as the best amount of adsorbent.

Effect of ionic strength on the removal efficiency of Ponceau 4R. The effect of ionic strength on the dye adsorption efficiency was investigated by addition 0, 0.05 and 0.1 M of NaCl. The results showed that with the increase in NaCl concentration, the adsorption capacity of NH$_2$-MMNCs is decreased significantly. Thus, the strategy of no salt addition was performed for the kinetic and isotherm studies. According to the results, the presence of high ionic content in the sample reduces removal efficiency.

Effect of pH on the removal efficiency of Ponceau 4R. One of the main factors influencing the capacity of adsorbent is solution pH. The productivity of adsorption is dependent on the solution pH, because variation in pH causes to change in the degree of ionization of the adsorptive molecule and the surface properties of adsorbent [18]. The pH of the solution was adjusted with adding either HCl or NaOH. The maximum adsorption capacity of Ponceau 4R is recorded at acidic pHs (pH = 2-3). After studying pH values of 2.0, 3.0 and 4.0, pH 2 was selected for all further adsorption experiments. At this pH, Ponceau 4R is properly adsorbed onto the surface of NH$_2$-MMNCs. At acidic pHs, amine groups have positive charges and can be linked to anionic dye *via* electrostatic interaction.

After obtaining optimum conditions for removal of Ponceau 4R, the additional tests were carried out to confirm the optimal conditions. The confirmation test was carried out in optimal conditions (pH = 2, adsorbent amount = 80 mg, stirring time = 30 min and without addition of salt) and the dye removal efficiency was obtained as 98.3%.

STUDY OF ADSORPTION ISOTHERM AND KINETIC

Dye Adsorption Kinetics

The kinetic study of Ponceau 4R adsorption onto NH$_2$-MMNCs is required for selecting the optimum operating conditions for the full-scale batch processes. Kinetic study was carried out to determine the rate of Ponceau removal by NH$_2$-MMNCs. For this purpose, a series of dye solutions with the same initial concentration of 50 and 100 mg l^{-1} under optimal condition was studied. The mixture were stirred in times ranging 0-90 min. Afterwards, the optical absorbance of clear supernatant solutions were examined in certain sampling times (0-5 min each one minute, 10-35 min each 5 min, 60 and 90 min) and measured using spectrophotometer at $\Lambda = 505$ nm for obtaining Ponceau 4R concentration in the solution. Figure 6a shows the effect of time on the Ponceau 4R removal. The removal rate was very

Table 1. Experimental Design

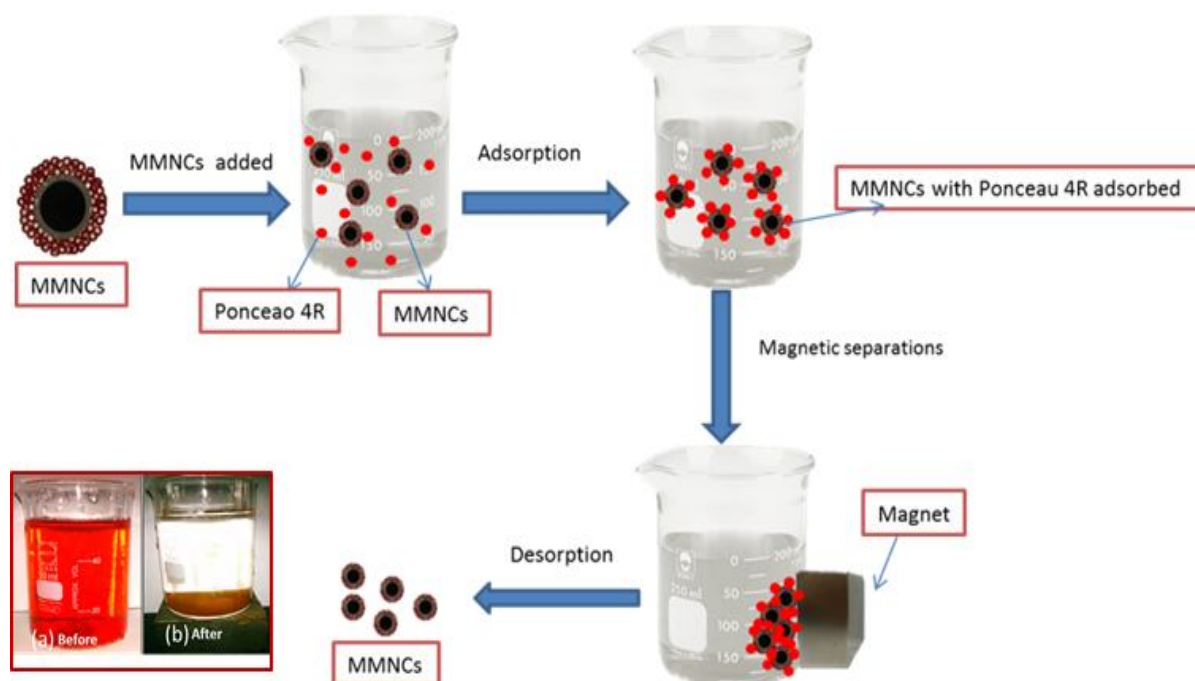| Number of test	Weight of adsorbent (g)	Ionic strength (M)	Stirring time (min)	pH
1	0.04	0.10	8	3
2	0.08	0.10	15	2
3	0.01	0.10	30	4
4	0.01	0.00	8	2
5	0.04	0.00	15	4
6	0.01	0.05	15	3
7	0.04	0.05	30	2
8	0.08	0.00	30	3
9	0.08	0.05	8	4

Fig. 5. A schematic diagram of the magnetic separation process for removal of Ponceau 4R (V = 50 ml, C = 50 mg l^{-1}, pH = 2, adsorbent amount = 80 mg and without addition of salt).

Table 2. Pseudo First Order ,Pseudo Second Order, Intra Particle Kinetic Models Parameters
for the Removal of Ponceau 4R by NH_2-MMNCs at Two Initial Concentrations of
Ponceau 4R (mg l^{-1}): (a) 100 mg l^{-1} of Ponceau 4R (b) 50 mg l^{-1} of Ponceau 4R

Table 2a. 100 mg l^{-1} of Ponceau 4R

Kinetic model	R^2	Equation	Constant	Values
First order	0.0275	$\log(q_e - q_t) = \log(q_e) - \dfrac{k_1}{2.333}t$	K_1	0.010
			q_e	3.349
Second order	0.9993	$\dfrac{t}{q_t} = \dfrac{1}{k^2 q_e^{~2}} + \left(\dfrac{1}{q_e}\right)t$	q_e	58.823
			K_2	0.067
Intra particle	0.3152	$q_t = k_{dif}\, t^{0.5} + C$	C	40.466
			k	3.3212

Table 2b. 50 mg l^{-1} of Ponceau 4R

Kinetic model	R^2	Equation	Constant	Values
First order	0.0042	$\log(q_e - q_t) = \log(q_e) - \dfrac{k_1}{2.333}t$	K_1	0.0039
			q_e	1.1530
Second order	0.9992	$\dfrac{t}{q_t} = \dfrac{1}{k^2 q_e^{~2}} + \left(\dfrac{1}{q_e}\right)t$	q_e	28.7300
			K_2	0.0670
Intra particle	0.1982	$q_t = k_{dif}\, t^{0.5} + C$	C	22.4000
			k	1.2800

fast during the initial stages of the adsorption processes (Table 2). At long times (60 and 90 min) the extraction efficiency was slightly reduced that can be related to the desorption of Ponceau 4R from the surface of NH_2-MMNCs. The kinetics data were analysed using pseudo first-order, pseudo second-order and intraparticle diffusion kinetic models. The kinetic rate was calculated according to the following equation [19-21]:

$$\frac{t}{q_t} = \frac{1}{k^2 q_e^{~2}} + \left(\frac{1}{q_e}\right)t \tag{2}$$

where k is the pseudo-second order rate constant. q_e and q_t

are the quantity of Ponceau 4R adsorbed (mg g^{-1}) at equilibrium and at each time, respectively.

The pseudo-first-order rate equation is equal:

$$\log(q_e - q_t) = \log(q_e) - \frac{k_1}{2.333}t \qquad (3)$$

where k_1 is the rate constant of pseudo first-order adsorption (min^{-1}), and q_e and q_t are the amounts of Ponceau 4R adsorbed (mg g^{-1}) at equilibrium and at time t (min), respectively. The results showed that kinetic data were fully fitted to the pseudo-second order kinetic model (Fig. 6b) suggesting chemisorption mechanism. The equilibrium adsorption capacity was obtained as 58.8 mg g^{-1}. The linear correlation coefficient value ($R^2 = 0.9993$) was found to be adequate.

Dye Adsorption Isotherm

The adsorption isotherms are important from both theoretical and practical points of view. In order to optimize the design of an adsorption system for dye removal, it is important to establish the most appropriate correlations of
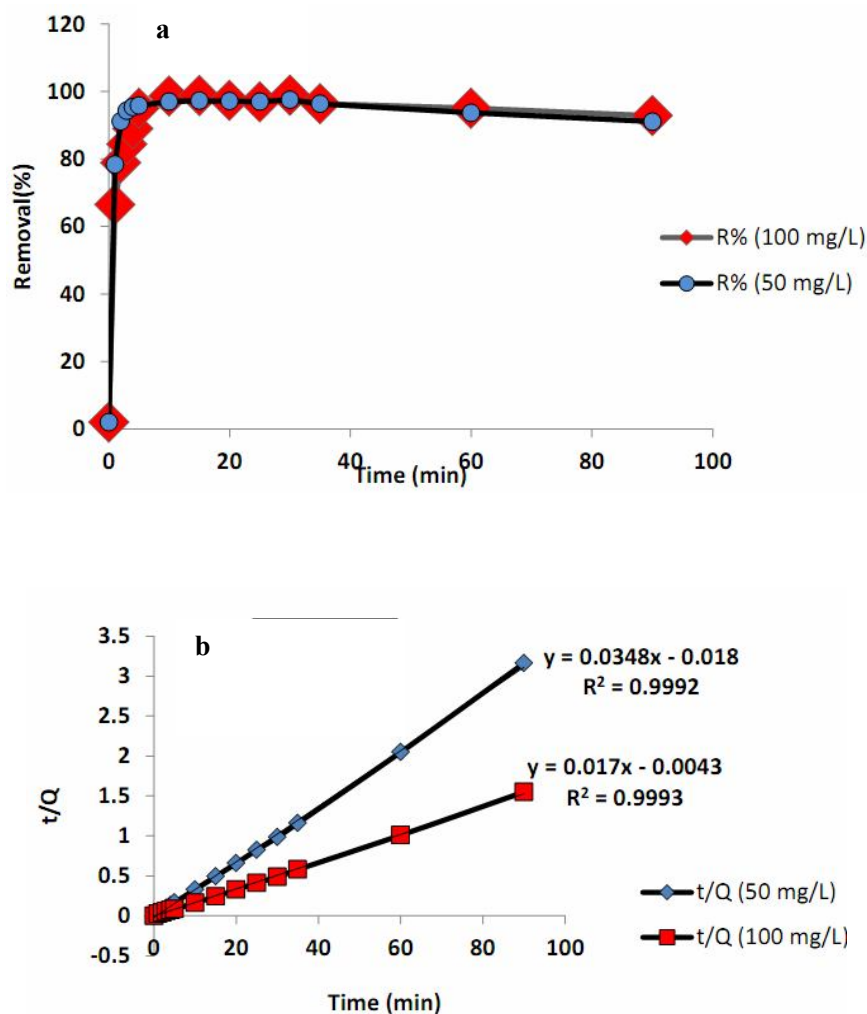

Fig. 6. (a) Effect of time on the removal efficiency of Ponceau 4R. (b)Pseudo-second order kinetic model (V = 50 ml, C = 50, 100 mg l^{-1}, pH = 2, adsorbent amount = 80 mg).
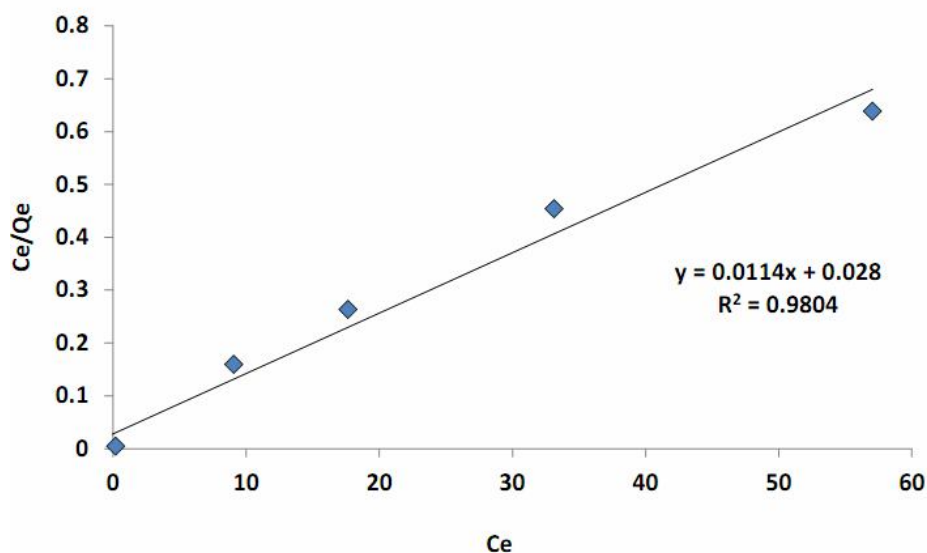
Fig. 7. Langmuir isotherm model (V = 50 ml, C = 25, 50, 75, 100, 125, 150 mg l^{-1}, pH = 2, adsorbent amount = 80 mg, stirring time 30 min and without addition of salt).

the equilibrium data of each system. In this study, the two most common isotherms, Langmuir and Freundlich models [22], were used to describe the experimental adsorption data. The fitting of data for dye sorption onto the NH$_2$-MMNCs suggesting that the Langmuir model with R^2 = 0.98 (Fig. 7) gives a better fit than the Freundlich model (R^2 = 0.50). The fit of the Langmuir model in the present system shows the formation of a monolayer covering of the adsorbate at the outer surface of the adsorbent. According to the results, Q$_{max}$, the maximum monolayer capacity of the sorbent (mg g^{-1}), and K$_L$, the Langmuir binding constant which is related to the energy of adsorption (l mg^{-1}), were obtained as 87.7 and 0.407, respectively (Table 3).

$$\frac{C_e}{q_e} = \frac{1}{kL\,q_{max}} + \frac{1}{q_{max}}C_e \qquad (4)$$

A simple regeneration study was conducted under optical condition to evaluate the reusability of the synthesized NH$_2$-MMNCs for dye removal. The results of consecutive usage of NH$_2$-MMNCs showed effective regeneration of magnetite nanoparticles even after four cycles of elution/adsorption.

REAL WATER SAMPLES

To verify the applicability and reliability of the proposed specified method for Ponceau 4R removal, three different samples, were collected from three main sources in Guilan Province in Iran (waste waters from Iran Barak and Chouka industries; well water from Salkisar village). Ponceau 4R was spiked to the water samples in such a way that the final concentrations of Ponceau 4R were fixed at 50 mg l^{-1}. All analyses were carried out under optimized conditions (pH = 2, adsorbent amount = 80 mg, stirring time = 30 min and without addition of salt). The analyte concentrations before and after removal process were determined by UV-Vis spectrophotometer. Table 4 shows the result of removal efficiency of Ponceau 4R in real water samples.

CONCLUSIONS

Dye removal from aqueous solutions plays a significant role in water pollution control. In this study, well-ordered amine functionalized Kit-6 mesoporous magnetite nanocomposites were chemically synthesized. The synthesized nanocomposites showed good crystallographic

Table 3. Langmuir and Freundlich Isotherm Model Parameters for the Removal of Ponceau 4R by MMNCs

Isotherms	Langmuir isotherm			Freundlich isotherm		
Parameters	R^2	Q_m	K_L	R^2	K_F	N
Values	0.9804	87.7	0.407	0.507	34.89	4.9

Table 4. Result of Removal Eefficiency of Ponceau 4R in Real Water Samples

Sample	$E\% = \dfrac{C_0 - C_{eq}}{C_0} \times 100$ Removal efficiency
Waste water of Iran Barak	94%
Waste water of Chouka	72%
Well water of Salkisar village	100%

order and large uniform pore size. Surface functionalization with amine groups produces good properties to adsorb Ponceau 4R via electrostatic interactions. The synthesized NH$_2$-MMNCs can be easily regenerated and reused for successive removal processes with high removal efficiency. The data reported here should be useful for the design and fabrication of an economically treatment process using batch (or) stirred tank reactors for dye adsorption. Due to their very high surface areas, high sorption capacity can be achieved in short exposure times.

ACKNOWLEDGMENTS

REFERENCES

[1] E. Dinc, E. Baydan, M. Kanbur, F. Onur, Talanta 58 (2002) 579.

[2] T. Tanaka, Food Chem. Toxicol. 44 (2006) 1651.

[3] J.S. Piccin, M.L.G. Vieira, J.O. Goncalves, G.L. Dotto, L.A.A. Pinto, J. Food Eng. 95 (2009) 16.

[4] S. Tsuda, M. Murakami, N. Matsusaka, K. Kano, K. Taniguchi, Y. Sasaki, Toxicol. Sci. 61 (2001) 92.

[5] C. Hessel, C. Allegre, M. Maisseu, F. Charbit, P. Moulin, J. Environ. Manage. 83 (2007) 171.

[6] J.F. Gao, Q. Zhang, J.H. Wang, X.L. Wu, S.Y. Wang, Y.Z. Peng, Bioresource Technol. 102 (2011a) 805.

[7] A.K. Verma, R.R. Dash, P.A. Bhunia, J. Environ. Manage. 93 (2012) 154.

[8] Y.L. Gao, C.M. Li, J.Y. Shen, H.X. Yin, X.L. An, H.Z. Jin, J. Food Sci. 76 (2011b) T125.

[9] S. Kobylewski, M.F. Jacobson, Int. J. Occupational Environ. Health 18 (2012) 220.

[10] G. Crini, P.M. Badot, Prog. Poly. Sci. 33 (2008) 399.

[11] T. Robinson, G. McMullan, R. Marchant, P. Nigam, Bioresource Technol. 77 (2001) 247.

[12] M. Khabazipour, S. Shariati, F. Safa, Syn. React. Inorg. Met. 46 (2016) 759.

[13] V. Janaki, K. Vijayaraghavan, B.-T. Oh, K.-J. Lee, K. Muthuchelian, A.K. Ramasamy, S. Kamala-Kannan, Carbohyd. Polym. 90 (2012) 1437.

[14] H. Kefayati, S.J. Bazargard, P. Vejdansefat, S. Shariati, A.M. Kohankar, Dyes Pigments 125 (2016)

309.

[15] A. Khorshidi, S. Shariati, RSC Adv. 4 (2014) 41469.

[16] F. Bandari, F. Safa, S. Shariati, Arab. J. Sci. Eng. 40 (2015) 3363.

[17] M.A.M. Salleh, *et al.*, Desalination 280 (2011) 1.

[18] B. Nandi, A. Goswami, M. Purkait, Appl. Clay Sci. 42 (2009) 583.

[19] S. Mohan, N. Rao, J. Kartikeyan, J. Hazard. Mater. B 90 (2002) 189.

[20] Y. Ho, G. McKay, Chem. Eng, J. 70 (1998) 115.

[21] I. Kiran, T. Akar, A. Özcan, A. Özcan, S. Tunali, Biochem. Eng. J. 31 (2006) 197.

[22] Y. Hamzeh, A. Ashori, E. Azadeh, A. Abdulkhani, Mater. Sci. Eng. C. 32 (2012) 1394.